https://doi.org/10.1038/s44298-026-00179-4

Immunogenicity and protective efficacy of MERS CoV, NL140422, and HKU4 spike protein nanoparticle vaccines

Check for updates

Peter J. Halfmann[1,8], Jeong Soo Lee[2,8], Tong Wang[1,8], Augustine Duffy[2,3,8], Yoshihiro Kawaoka[1,4,5,6] ✉ & Ravi S. Kane[2,3,7] ✉

While vaccines against Middle East respiratory syndrome coronavirus (MERS-CoV) have had substantial preclinical and clinical development, few vaccine candidates target other related viruses with potential for human spillover within the *Merbecovirus* subgenus, like NL140422 and HKU4. We designed nanoparticle vaccines displaying the spike ectodomains of MERS-CoV, NL140422, and HKU4 and evaluated their immunogenicity and protective efficacy in mice. All vaccines elicited high IgG antibody titers against the corresponding vaccine spike protein with moderate cross-binding to mis-matched spike proteins as well. Only the MERS-CoV spike protein induced detectable neutralizing antibodies against MERS-CoV. In human dipeptidyl peptidase 4 (hDPP4) transgenic mice, vaccination with MERS-CoV spike protein completely inhibited MERS-CoV replication in the lungs and nasal turbinates. Vaccination with NL140422 and HKU4 spike proteins provided partial but significant reductions of lung viral loads after MERS-CoV challenge, highlighting their utility as components of a future pan-*Merbecovirus* vaccine.

Since the turn of the 21st century, three pathogenic coronaviruses have emerged in human circulation: SARS-CoV in 2002, MERS-CoV in 2012, and SARS-CoV-2 in 2019. The COVID-19 pandemic caused by SARS-CoV-2 underscored the need for universal coronavirus vaccines against not only these three pathogenic human coronaviruses but also against closely related coronaviruses in animal reservoirs with the potential to spill over to humans. While much work has been done to design vaccines against SARS-CoV-2, SARS-CoV, and their related viruses known as sarbecoviruses, the development of vaccines against MERS-CoV and its related viruses, known as merbecoviruses, has been more limited.

MERS-CoV, the only known merbecovirus to have infected humans, emerged in 2012 and was isolated from a patient in Saudi Arabia[1]. Like the other pathogenic coronaviruses that cause disease in humans, MERS-CoV is an enveloped positive-sense single-stranded RNA coronavirus that binds to and infects cells through its spike (S) protein and infects respiratory tissues. Unlike SARS-CoV and SARS-CoV-2 spike proteins that bind to the angiotensin-converting enzyme 2 (ACE2) as the host receptor, MERS-CoV spike proteins instead recognize hDPP4 and use it as an entry receptor. The human case fatality rate of MERS, the disease caused by MERS-CoV, is quite high at 36%, and the virus continues to circulate among dromedary camels in the Middle East, posing a continuing threat of further spillover to humans[2].

The development of MERS-CoV vaccines has been a high priority both to address the current threat of spillover as well as to guard against future pandemics. Several MERS-CoV vaccines have undergone early stage clinical trials, such as a Chimpanzee Adenovirus Oxford 1-vectored spike protein vaccine[3], modified vaccinia virus Ankara-vectored spike protein vaccine[4], and an electroporation-delivered DNA spike protein vaccine[5]. Many more MERS-CoV vaccines are in preclinical development, such as vaccines delivered as soluble protein[6–10], as Fc fusion proteins, on protein nanoparticles[11–14], on polymeric nanoparticles[15], on bacterial outer membrane vesicles[16], as free or encapsulated DNA[17], as mRNA in lipid nanoparticles[18], or via viral vectors[19].

However, while many studies have worked to develop vaccines against MERS-CoV, few have attempted to design vaccines against other

[1]Department of Pathobiological Sciences, Influenza Research Institute, School of Veterinary Medicine, University of Wisconsin, Madison, WI, USA. [2]School of Chemical & Biomolecular Engineering, Georgia Institute of Technology, Atlanta, GA, USA. [3]Parker H. Petit Institute for Bioengineering and Bioscience, Georgia Institute of Technology, Atlanta, GA, USA. [4]Division of Virology, Department of Microbiology and Immunology, Institute of Medical Science, University of Tokyo, Tokyo, Japan. [5]The Research Center for Global Viral Diseases, National Center for Global Health and Medicine Research Institute, Tokyo, Japan. [6]Pandemic Preparedness, Infection and Advanced Research Center (UTOPIA), University of Tokyo, Tokyo, Japan. [7]Wallace H. Coulter Department of Biomedical Engineering, Georgia Institute of Technology, Atlanta, GA, USA. [8]These authors contributed equally: Peter J. Halfmann, Jeong Soo Lee, Tong Wang, Augustine Duffy. ✉e-mail: yoshihiro.kawaoka@wisc.edu; ravi.kane@chbe.gatech.edu

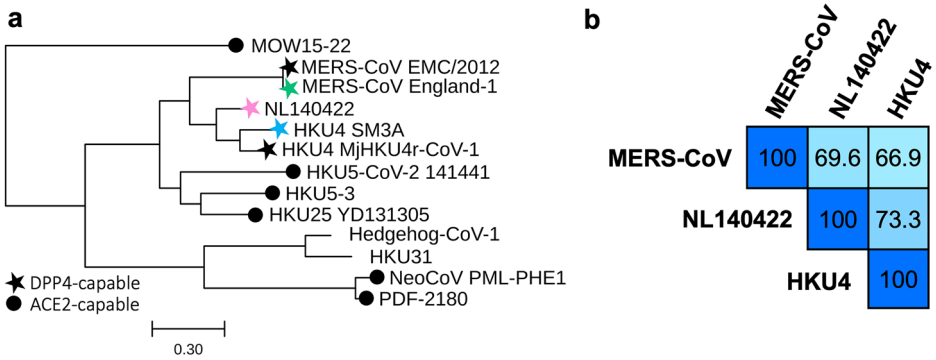

Fig. 1 | Phylogenetic and sequence analysis of Merbecovirus S proteins. a Phylogenetic tree of representative *Merbecovirus* S protein sequences. Colored stars denote the virus strains chosen as antigenic components in the VLP-S vaccines. Scale bar represents the number of mutation events per residue. **b** Pairwise sequence identity matrix of S proteins used for immunization. The intensity of blue shading reflects the degree of sequence similarity, with darker colors indicating higher percentage identity.

merbecoviruses, particularly other merbecoviruses that use DPP4 such as NL140422 and HKU4[20–30]. NL140422 virus was first identified in 2014 from samples collected from the great evening bat (*Ia io)* in Guangdong Province, China[24], and has been shown to efficiently infect human cells via hDPP4 following protease treatment[25]. The HKU4 lineage is primarily bat-derived, and three members, MjHKU4r-CoV-1, Pangolin-CoV-HKU4-P251T, and Ty-BatCoV HKU4 SM3A, have also been reported to efficiently infect human cells[26–28]. Our group has previously developed vaccines displaying just the S2 subunit from the spike proteins of the merbecoviruses HKU4, HKU25, and NeoCoV based on a stabilized MERS-CoV S2[31], and we evaluated their efficacy against MERS-CoV challenge in a mouse model[32]. However, while S2 vaccines may induce antibodies against conserved epitopes on the spike protein, S2-directed vaccines tend to elicit a weaker neutralizing antibody response than vaccines encoding the full spike protein. Accordingly, we here designed nanoparticle vaccines displaying the full, stabilized spike protein ectodomains from the DPP4-using merbecoviruses MERS-CoV, NL140422, and HKU4 and evaluated their immunogenicity and protective efficacy in a mouse model.

Results

Merbecovirus strain selection for vaccine immunization

We focused on merbecoviruses capable of utilizing hDPP4, with the long-term goal of designing broadly protective vaccines against this group of viruses. The candidate selection was guided by the *Merbecovirus* phylogeny (Fig. 1a), which highlighted MERS-related coronavirus, NL140422, and HKU4 as hDPP4-utilizing target lineages[20–23,26–30]. Selection was further refined based on the likelihood of cross-reactive response and zoonotic transmission. MERS-CoV was included owing to its ongoing circulation and high mortality rate, with the England-1 strain chosen as the representative virus for S antigen design. HKU4 was also incorporated, represented by the SM3A strain. At the time of study initiation (May 2023), HKU4 SM3A was the only lineage member confirmed to infect human cells, as reports of Pangolin-CoV-HKU4-P251T infectivity were not yet available and the genome of MjHKU4r-CoV-1 had not been published[26–30].

The S protein amino acid sequence homology (Fig. 1b) was analyzed to assess potential cross-reactivity among the vaccine candidates. Each S protein, designed from one of the three representative merbecoviruses, was evaluated for sequence identity against the others. The three viruses exhibited comparable S protein sequence conservation, with percent identities differing by less than 10%, suggesting a likelihood of similar vaccine-elicited cross-reactive antibody responses. Notably, NL140422 demonstrated the highest sequence identity against the other two S proteins, indicating its potential to elicit the most broadly cross-reactive antibody response.

Assembly and in vitro characterization of VLP-S vaccines

Previously, our group designed VLP vaccines displaying full S and S2 subunits on streptavidin (SA)-coated MS2 nanoparticles (MS2-SA)[32–36]. Briefly, the VLP core consists of 90 homodimers of the bacteriophage MS2 coat protein, engineered to contain an AviTag within a surface-exposed loop. These coat proteins self-assemble into an icosahedral structure. In this study, we employed the same VLP platform to multivalently present S proteins on the MS2-SA scaffold (Fig. 2a). Following expression, the Avi-Tagged MS2 VLPs were enzymatically biotinylated and mixed with an excess of tetrameric streptavidin to produce MS2 particles densely coated with streptavidin (MS2-SA). S proteins, each containing a C-terminal trimerization motif, AviTag, and hexahistidine tag, were expressed in Expi293F mammalian cells. Purification was performed using immobilized metal affinity chromatography (IMAC), followed by in vitro biotinylation and further purification by size exclusion chromatography (SEC) (Fig. 2b). The SEC chromatogram confirmed the trimerized state of the S proteins. Final VLP-S particles were assembled by combining MS2-SA with biotinylated S protein at an optimized ratio. This ratio was determined by SEC to be the lowest amount of MS2-SA that avoided generating a peak corresponding to unbound excess S protein.

Comprehensive characterization of the final VLP-S vaccine constructs was performed using dynamic light scattering (DLS), SDS polyacrylamide gel electrophoresis (SDS-PAGE), and enzyme-linked immunosorbent assay (ELISA). DLS measurements showed that the S proteins had an average diameter of approximately 20 nm. Upon multivalent display on MS2-SA, which measured diameters of 40–45 nm, the resulting VLP-S constructs measured approximately 90 nm in diameter (Fig. 2c). This measurement is consistent with measurements from our previous VLP-S vaccines[33,35]. SDS-PAGE analysis verified the purity across all protein components within the VLP-S constructs (Fig. 2d). To enable accurate molecular weight comparisons, PNGase F treatment was used to remove N-glycans from the S protein (Fig. 2d). Additionally, heated VLP-S samples were analyzed alongside BSA standards on SDS-PAGE to estimate antigen valency, revealing that each VLP particle displayed approximately 22 S molecules (Supplementary Fig. 3). To verify the conformational integrity of antigenic sites on the S proteins, ELISAs were conducted with two MERS-CoV RBD-specific monoclonal antibodies (CDC2-C2 and m336) and a cross-reactive S2-specific monoclonal antibody (S2P6) (Fig. 2e and Supplementary Fig. 4). Binding profiles indicated that the VLP-displayed S proteins maintained proper folding and presentation of key epitopes.

VLP-S immunization

Five female C57BL/6 mice, aged 6-8 weeks, were immunized subcutaneously with each VLP-S vaccine (VLP-MERS-CoV S, VLP-NL140422 S, VLP-HKU4 S) or VLP-Control (MS2-SA), adjuvanted with Alhydrogel (Fig. 3a). Each vaccine dose presented 7.5 μg of S antigen on the MS2-SA scaffold. Humoral responses were assessed by measuring IgG endpoint titers against the S proteins of MERS-CoV, NL140422, and HKU4 (Fig. 3b). All vaccinated mice developed antibodies that recognized not only the spike protein used for immunization but also the other two merbecovirus spike proteins, with the strongest titers observed against the homologous spike protein.

To visualize the antigenic relationships among the vaccine candidates, we constructed an antigenic map using IgG endpoint titers (Fig.

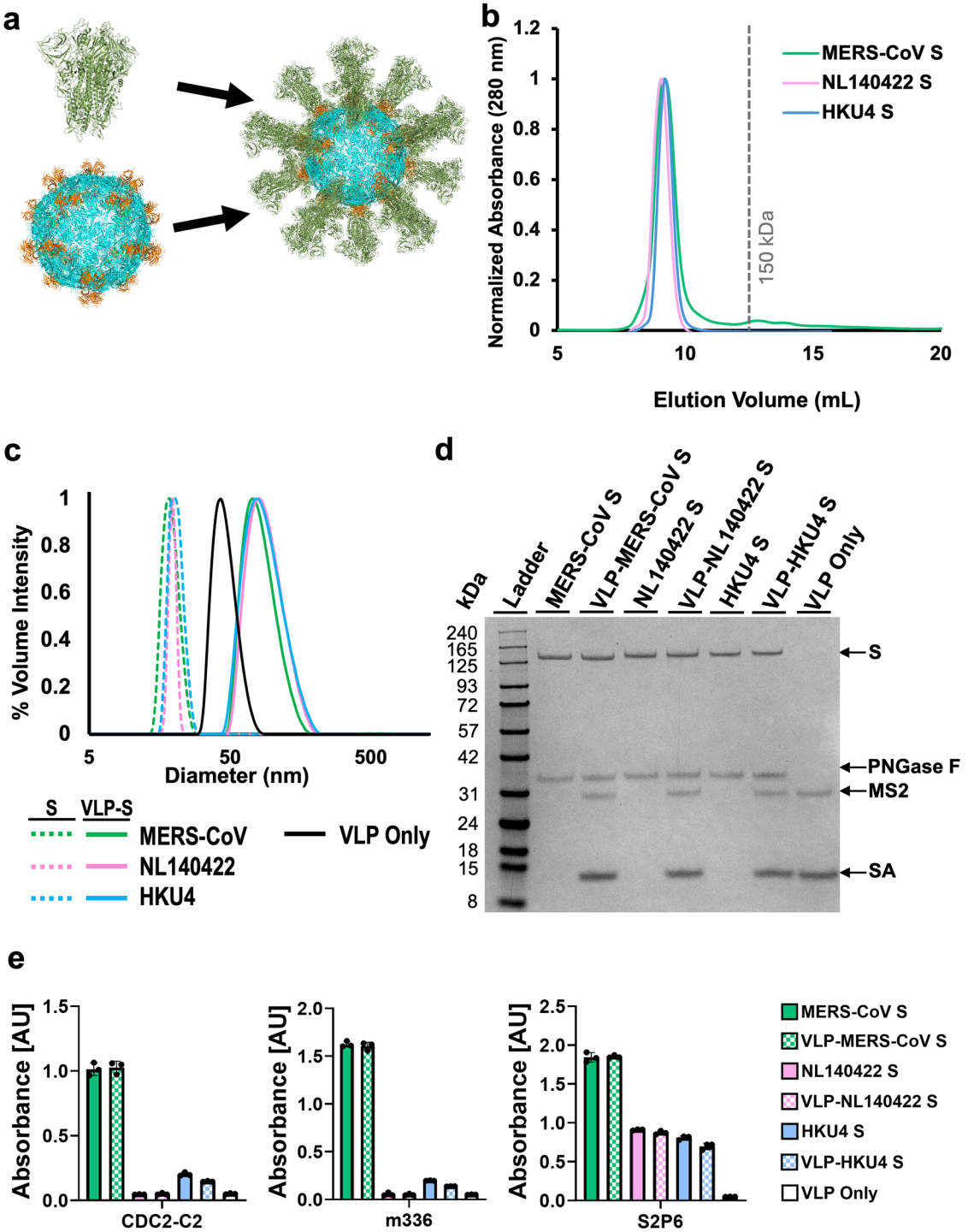

Fig. 2 | Characterization of S antigens and VLP-S constructs. a Schematic of the S protein (green, PDB: 5×58), MS2-SA (MS2: cyan, PDB: 2MS2; SA: orange, PDB: 3RY2) and VLP-S. **b** Size exclusion chromatography curves for S proteins. The vertical gray line represents the peak elution volume of the molecular weight standard γ-globulin (150 kDa, Millipore Sigma). The column void volume is 8 mL. **c** Characterization of S, MS2-SA, and VLP-S by dynamic light scattering. **d** Sodium dodecyl sulfate-polyacrylamide gel electrophoresis (SDS-PAGE) characterization of S and VLP-S. The unprocessed gel is shown in Supplementary Fig. 1. **e** Enzyme-linked immunosorbent assay (ELISA) characterization of the binding of CDC2-C2, m336, and S2P6 antibodies to S proteins and VLP-S constructs. (mean ± SD, $n = 3$: one assay with three technical replicates).

3c). Although such maps are traditionally derived from functional assays like hemagglutination inhibition or neutralization assays, antigenic cartography can also be applied to binding data to infer relative antigenic similarity[32,37]. Following a similar approach, we constructed a map based on binding titers. We observed a triangular antigenic landscape with relatively uniform endpoint titers across all sera, indicating relatively balanced reactivity. The shortest leg of the triangle appears to be between the MERS-CoV antigen and sera groups (green) and the NL140422 antigen and sera groups (pink). The sera from VLP-NL140422 S immunized mice (pink squares) do appear closer to the MERS-CoV ELISA antigen (green circle) than the VLP-MERS-CoV S sera (green squares) are to the NL140422 antigen (pink circle),

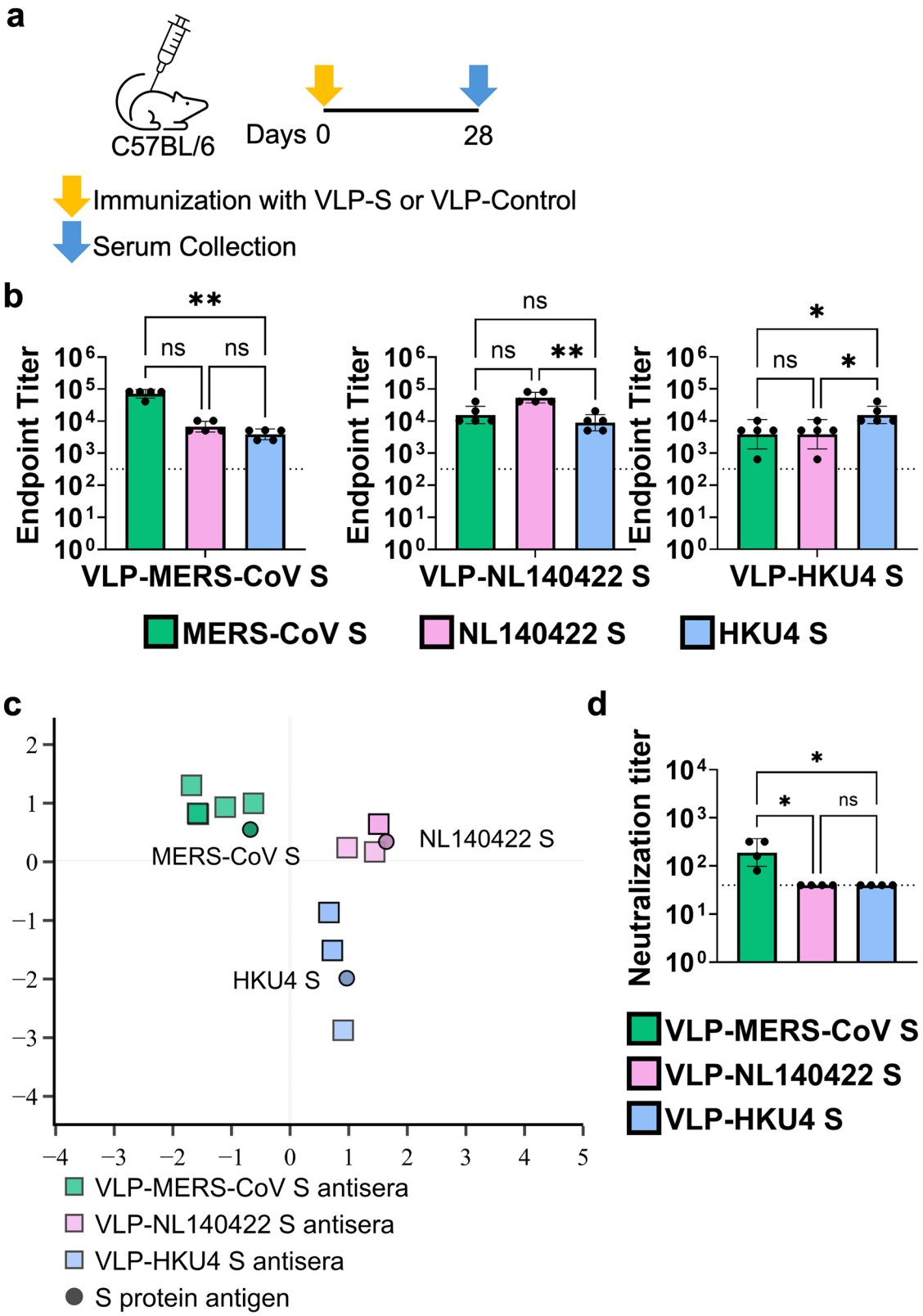

indicating that the VLP-NL140422 S vaccine may be more suitable as a single vaccine candidate against these two targets than VLP-MERS-CoV S would be, though the insignificant differences in absolute ELISA titer may render this distinction unnecessary. Regardless, MERS-CoV and NL140422 spike proteins appear to be more antigenically similar to each other than either is to HKU4, suggesting that any mixture vaccine seeking to cover the DPP4-utilizing merbecovirus space would likely require an HKU4 antigen and at least one of MERS-CoV or NL140422.

A neutralization assay based on virus-induced cytopathic effect was used to evaluate the elicited antibodies for the three vaccine groups. As shown in Fig. 3d, VLP-MERS-CoV S induced a modest level of neutralizing antibodies against MERS-CoV. Although IgG antibody titers elicited by

Fig. 3 | Characterization of antibody responses and neutralization titers for sera from C57BL/6 mice immunized with VLP-S vaccines. a Schematic of immunization schedule. **b** IgG endpoint titers against S proteins from MERS-CoV (green), NL140422 (pink), and HKU4 (blue) following a single dose of VLP-MERS-CoV S, VLP-NL140422 S, or VLP-HKU4 S. Black dots represent data from an individual mouse (geometric mean with geometric SD, $n = 5$: sera from 5 mice). $^{**}P < 0.01$, $^{*}P < 0.05$, ns: not significant, determined by Kruskal-Wallis test with Dunn's multiple comparisons test. The limit of detection (dotted line) is a serum dilution of 1:320. **c** Antigenic map constructed using IgG endpoint titers from sera of five mice per vaccinated group. Each square represents an individual mouse serum sample, and black dots denote S protein antigens. Each square is color-coded according to the vaccine group (VLP-MERS-CoV S: green; VLP-NL140422 S: pink; VLP-HKU4 S: blue). Antisera at overlapping positions are indicated with darker shaded squares and colored dots and a text label identify the viral antigen (MERS-CoV S: green; NL140422 S: pink; HKU4 S: blue). Distances between points are expressed in antigenic units, where 1 unit equals a twofold dilution difference in antibody titer. **d** MERS-CoV neutralization titers at 1000 plaque-forming units (pfu) (VLP-MERS-CoV S: green; VLP-NL140422 S: pink; VLP-HKU4 S: blue). Endpoint titers were determined using 2-fold serial dilution of sera and reported as the reciprocal of the highest dilution that showed complete inhibition of cytopathic effects. Black dots represent data from an individual mouse (geometric mean with geometric SD, $n = 4$: sera from 4 mice). Statistical analysis performed using Kruskal-Wallis test with Dunn's multiple comparisons test ($^{*}P < 0.05$, ns not significant). The limit of detection (dotted line) is a serum dilution of 1:40.

VLP-NL140422 S and VLP-HKU4 S showed cross-reactive binding to the MERS-CoV S protein, no neutralizing antibodies against MERS-CoV were detected with sera from either of these vaccine groups.

VLP-S vaccines provide partial cross-protection against MERS-CoV

The protective efficacy of the VLP-S vaccines was assessed in transgenic hDPP4 mice through a challenge study. Groups of five female mice aged 6-8 weeks were immunized once with the VLP-S vaccines or VLP-Control (MS2-SA), each formulated with Alhydrogel adjuvant (Fig. 4a). Four weeks following immunization, mice were challenged intranasally with 10^5 plaque-forming units (pfu) of MERS-CoV. As viral titers in hDPP4 mice typically begin to decline at three days post-infection[38,39], lung and nasal turbinate tissues were harvested on day 3 post-challenge to quantify viral loads using standard plaque assays on Vero E6 stably expressing human TMPRSS2 (Vero E6/TMPRSS2) cells.

Mice from all three vaccine groups exhibited significantly reduced lung viral titers following MERS-CoV challenge compared to the control group (Fig. 4b). Mice immunized with VLP-NL140422 S and VLP-HKU4 S demonstrated partial cross-protection against MERS-CoV, showing 2.5 and 1.7 log reductions in lung viral titers compared to the control group, respectively. No significant reduction in viral titers was observed in the nasal turbinates of mice vaccinated with VLP-NL140422 S or VLP-HKU4 S. Immunization with VLP-MERS-CoV S conferred full protection from MERS-CoV challenge in mice as indicated by undetectable levels of virus in the lungs and nasal turbinates (Fig. 4b, c).

Discussion

We generated VLP vaccines presenting the S proteins of MERS-CoV, NL140422, and HKU4 to evaluate cross-lineage immune responses among hDPP4-utilizing merbecoviruses. Each vaccine induced strong antigen-specific and cross-reactive IgG responses in mice. As expected, IgG antibody titers were highest against the homologous antigen. Interestingly, immunization with VLP-NL140422 S produced stronger IgG antibody responses against MERS-CoV S than against HKU4 S, even though NL140422 shares slightly higher sequence identity with HKU4 (73.3%) than with MERS-CoV (69.9%). Antigenic mapping based on IgG antibody endpoint titers also showed limited serological overlap between VLP-MERS-CoV S and VLP-NL140422 S responses with HKU4 S. These observations suggest that overall sequence similarity does not necessarily reflect antigenic relationships and that features such as the conservation of immunodominant epitopes or structural conformation may play an important role.

When challenged with MERS-CoV, hDPP4 mice vaccinated with VLP-MERS-CoV S had undetectable virus titers in the lungs, while hDPP4 mice vaccinated with VLP-NL140422 S or VLP-HKU4 S had markedly reduced viral titers, demonstrating partial protection and limited cross-protection by the S protein of these viruses. Notably, VLP-NL140422 S produced a greater reduction in lung viral titers than VLP-HKU4 S, consistent with the serological data showing lower cross-reactivity of HKU4 S IgG antibodies with heterologous spikes. These findings suggest that the extent of cross-reactive antibody responses may influence protective outcomes. Despite this, vaccination with VLP-NL140422 S and VLP-HKU4 S failed to elicit neutralizing antibodies against MERS-CoV, implying that protection may be mediated by non-neutralizing antibodies such as those inducing Fc-mediated effector functions or by $CD8^+$ T-cell cytotoxicity. Clinical studies of a MERS-CoV S-based vaccine have demonstrated the induction of antibodies capable of mediating Fc-dependent effector functions, alongside spike-specific $CD8^+$ T-cell responses[40,41]. In parallel, extensive studies on SARS-CoV-2 vaccines have established Fc-mediated antibody functions and $CD8^+$ T-cell responses as important correlates of protection[42–44]. Accordingly, future work should include evaluations of antibody-dependent cellular cytotoxicity (ADCC) and antibody-dependent cellular phagocytosis (ADCP), as well as $CD8^+$ T-cell depletion studies, to determine the possible roles of Fc effector pathways or $CD8^+$ T-cell responses. Such analyses will help clarify the immune correlates of protection induced by VLP-S vaccination.

A limitation of the current study concerns the challenge experiments that could be performed. Cross-protective efficacy was assessed only against MERS-CoV, which precludes direct evaluation of protection against NL140422 or HKU4. Because additional challenge viruses were not available, we were unable to directly test protection across these lineages. Future studies incorporating reciprocal challenge models will be important for defining the breadth of protection across *Merbecovirus* lineages. Collectively, these findings help establish a framework for advancing vaccine strategies with broader protection against merbecoviruses.

Methods

Expression and purification of S antigens

DNA constructs encoding MERS-CoV England-1 S with the 2 P substitutions[45], NL140422 S with 2 P and A885P substitutions[25], and HKU4 SM3A S with 2 P and T985P substitutions were synthesized (Gene Universal, Newark, DE). Each sequence was fused to a T4 fibritin trimerization domain, AviTag, and C-terminal 6×His Tag, and cloned into pcDNA3.1(-). Expi293F cells (RRID: CVCL_D615) were transfected with the plasmids per manufacturer protocol via the ExpiFectamine Transfection Kit (Thermo Fisher Scientific). Supernatants were harvested 5 days post-transfection by centrifugation (6000 × *g*, 10 min), followed by two rounds of dialysis against 1×PBS (2 h each, with fresh buffer). Dialyzed supernatants were incubated overnight at 4 °C with HisPure Ni-NTA resin (1 mL, Thermo Fisher Scientific) under gentle stirring. The resin–protein mixture was loaded onto a gravity flow column (G-Biosciences), washed with 90 mL of binding buffer (150 mM Tris, 150 mM NaCl, 20 mM imidazole, pH 8), and eluted in three fractions using 3 mL of elution buffer (150 mM Tris, 150 mM NaCl, 400 mM imidazole, pH 8).

Eluates were concentrated to ~1 mL using a 10 kDa MWCO centrifugal filter (Millipore Sigma) and further purified by size-exclusion chromatography on a Superdex 200 Increase 10/300 column (Cytiva) equilibrated with PBS, monitored through absorbance at 280 nm, as described previously[32–36]. Protein concentrations were determined by bicinchoninic acid (BCA) assay (Thermo Scientific), where dosing is based on the amount of S included in each sample.

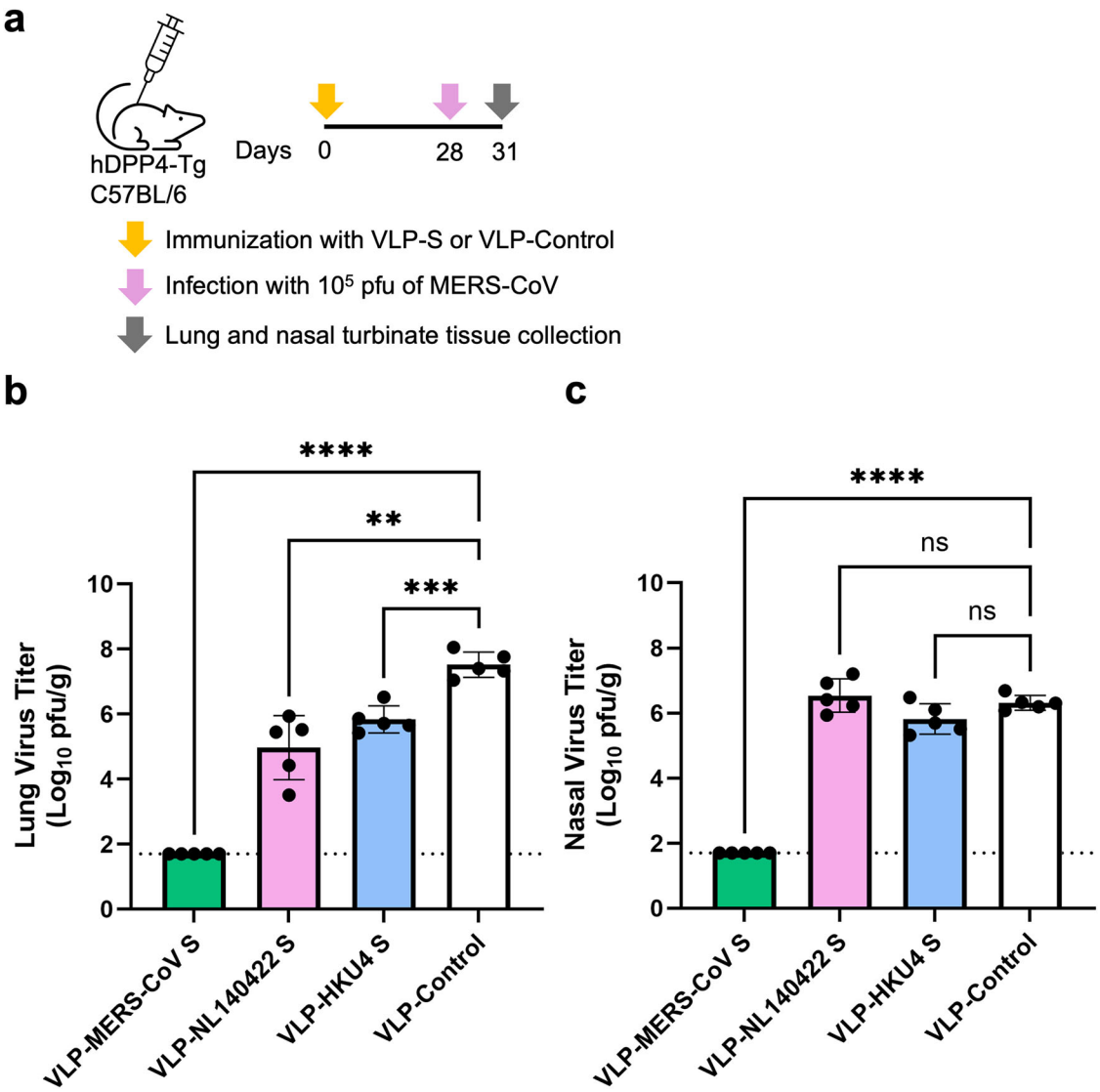

Fig. 4 | Protective efficacy of VLP-S vaccines. a Schematic diagram of the immunization schedule. Virus titers from the lung (**b**) and nasal turbinate (**c**) tissues of hDPP4 mice immunized with VLP-S or VLP-Control three days after infection with MERS-CoV (mean with SD, $n = 5$: tissue from 5 mice). ****$P < 0.0001$, ***$P < 0.001$, ** $P < 0.01$, ns – not significant determined by the Brown-Forsythe and Welch ANOVA test with Dunnett's T3 multiple comparisons test. The limit of detection (dotted line) is 1.7 $\log_{10}$ pfu/g.

Expression and purification of MS2

The gene encoding a single-chain MS2 coat protein dimer containing an AviTag insertion between residues 14 and 15 of the second monomer[33] was synthesized and cloned into pET-28b (GenScript Biotech, Piscataway, NJ). The plasmid was co-transformed with pAcm-BirA (Avidity LLC) into BL21(DE3) *E. coli* (New England Biolabs) following the manufacturer's protocol. Transformed cells were grown overnight at 37 °C in 5 mL of 2xYT medium and subsequently scaled to a 1 L culture. Cells were cultured at 37 °C with shaking at 225 rpm until reaching an OD600 of 0.6, at which point protein expression was induced with 1 mM IPTG (Fisher BioReagents) and supplemented with 50 nM D-biotin. Cultures were then shifted to 30 °C and incubated overnight. Cells were harvested by centrifugation (7000 × g, 7 min), and the pellet was resuspended in 25 mL lysis buffer (20 mM Tris, 0.5 mg/mL lysozyme, 125 units of EMD Millipore benzonase, one-quarter SigmaFast EDTA-free protease inhibitor tablet; pH 8). Suspensions were incubated on ice for 20 min, followed by addition of 0.1% (w/v) sodium deoxycholate. Cell disruption was performed by sonication (35% amplitude, 3 s pulses, 3 min) twice with a 5 min interval. Lysates were clarified by centrifugation (19,000 × *g*, 30 min), and the supernatant was diluted threefold before purification. Clarified lysates were passed through four HiScreen Capto Core 700 columns (Cytiva) connected in series and washed with five column volumes of 20 mM Tris (pH 8). The eluate was concentrated using a 10 kDa MWCO centrifugal filter and further purified by size-exclusion chromatography on a Superdex 200 Increase 10/300 column (Cytiva) equilibrated in TBS (20 mM Tris, 20 mM NaCl, pH 8). Final protein concentrations were determined by BCA assay (Thermo Fisher Scientific).

In vitro biotinylation of AviTagged S and MS2 proteins

The AviTag on MS2 and S protein was biotinylated using the BirA-500 kit (Avidity LLC) per manufacturer protocol. Briefly, 45 μM AviTagged protein was incubated with BirA ligase and Biomix B (biotin, ATP, and magnesium acetate) overnight at 4 °C. The same amount of Biomix B was added twice with a 2 h incubation at 37 °C in between and incubated overnight at 4 °C. The next morning, the mixture was run on a Superdex 200 Increase 10/300 column (Cytiva) to remove BirA and excess reagents. The concentration of biotinylated S and MS2 protein was measured by BCA assay.

Expression, refolding, and purification of streptavidin

The expression and purification of streptavidin (SA) followed established methods[32–36,46]. The SA gene (Addgene plasmid #46367, a gift from Mark Howarth) was transformed into BL21(DE3) cells. Four overnight starter cultures (5 mL, 2xYT) were scaled into 1 L 2xYT each and grown at 37 °C while shaking until OD600 reached 0.6. Expression was induced with 1 mM IPTG, and cultures were incubated overnight at 30 °C. Cells were harvested (7000 × g, 7 min) and resuspended in lysis buffer (50 mM Tris, 100 mM NaCl, pH 8.0) containing 1 mg/mL lysozyme (Alfa Aesar) and benzonase (500 units; EMD Millipore). After a 30 min incubation at 4 °C, lysis was performed by sonication (35% amplitude, 3 min, 3 s on, 3 s off) in the presence of 0.1% (w/v) sodium deoxycholate. The lysis process was repeated, but with benzonase excluded. The inclusion body pellets were homogenized, sonicated (35% amplitude, 30 s), and centrifuged (27,000 × *g*, 15 min) three times in 100 mL of washing buffer #1 (50 mM Tris, 100 mM NaCl, 100 mM EDTA, 0.5% (v/v) Triton X-100, pH 8.0). The pellet was then homogenized, sonicated (35% amplitude, 30 s), and centrifuged (15,000 × *g*, 15 min) three more times in 50 mL of washing buffer #2 (50 mM Tris, 10 mM EDTA, pH 8.0). Inclusion body pellets were solubilized in resuspension buffer containing 7.1 M guanidine hydrochloride, and the solution was incubated for an hour at room temperature. After centrifugation (12,000 × *g*, 12 min), the supernatant was transferred to a syringe and then added dropwise at a rate of 30 mL/hour to chilled 1 L PBS with vigorous stirring. After stirring the solution overnight at 4 °C, insoluble contaminants were removed by centrifugation (17,000 × *g*, 15 min) and the supernatant was filtered through a 0.45 µm bottle-top filter. Next, ammonium sulfate was slowly added to the rapidly stirring supernatant to a concentration of 1.9 M and mixed at 4 °C for 3 h to precipitate out impurities. After another round of centrifugation (17,000 × *g*, 15 min) and filtration, more ammonium sulfate was added to the supernatant up to a final concentration of 3.68 M. After overnight stirring at 4 °C, the solution was centrifuged (17,000 × g, 15 min) to pellet out SA. Pelleted SA was resuspended in 20 mL of Iminobiotin Affinity Chromatography (IBAC) binding buffer (50 mM sodium borate, 300 mM NaCl, pH 11.0) and purified on iminobiotin agarose resin (Thermo Scientific). The resin was washed with 10 CVs of binding buffer and SA was eluted with 4 CVs of elution buffer (20 mM potassium phosphate, pH 2.2). The eluate was dialyzed overnight into PBS at 4 °C, concentrated using a 10 kDa MWCO centrifugal filter, and quantified by absorbance at 280 nm.

Assembly and purification of MS2-SA VLP

The assembly of MS2-SA VLPs has been previously described[32–36]. A 20 × molar excess of SA was prepared in a small glass vial at ≥ 30 mg/mL, and MS2 at 700 µg/mL was added dropwise under rapid stirring. The resulting mixture was run on a Superdex 200 Increase 10/300 column equilibrated in PBS to separate free SA from assembled MS2-SA particles. To quantify the amount of SA within the VLP eluate, VLP samples were mixed with NuPAGE lithium dodecyl sulfate (LDS) sample buffer (Invitrogen), heated at 90 °C for 30 min, and resolved on a 4–12% Bis-Tris gel (Invitrogen). The gel included SA standards of known concentrations, and band intensities were compared to determine the amount of SA incorporated into MS2-SA VLPs.

Preparation of VLP-S

The stoichiometric ratio of MS2-SA to biotinylated S was optimized by analytical SEC. Fixed amounts of biotinylated S (8 µg) were incubated with varying quantities of MS2-SA and were run on SEC. The optimal ratio was defined as the lowest amount of MS2-SA that resulted in complete incorporation of S, as indicated by the absence of unbound S in the chromatogram.

Enzyme-linked immunosorbent assay (ELISA)

Nunc MaxiSorp 96-well flat-bottom plates (Invitrogen) were coated overnight at 4 °C with 0.2 µg S protein in 100 µL PBS per well. Plates were blocked with 200 µL PBST (PBS with 0.05% Tween-20) containing 5% (w/v) bovine serum albumin (BSA) for 1 h at room temperature. 100 µL of PBST with 1% BSA containing primary antibody m336 (2 nM), or CDC2-C2 (2 nM), or S2P6 (3 nM) was added to each well. After 1 hour, wells were washed three times with PBST and incubated for 1 h with 100 µL horseradish peroxidase–conjugated anti-human IgG Fc goat antibody (MP Biomedical, cat. #674171) at a 1:5000 dilution in PBST with 1% BSA. Following three washes, wells were developed with 100 µL TMB substrate solution (Thermo Scientific) for 2.5 min, and the reaction was stopped with 100 µL of 160 mM sulfuric acid. Absorbance at 450 nm was measured using a Synergy H4 plate reader with Gen5 2.07 software (BioTek).

Sodium Dodecyl Sulfate polyacrylamide gel electrophoresis (SDS-PAGE)

Samples containing either 1 µg S or 1 µg S displayed on assembled VLP-S were prepared. Proteins were deglycosylated using PNGase F (New England Biolabs) according to the manufacturer's denaturing reaction protocol. Following deglycosylation, samples were supplemented with 2 µL 2-mercaptoethanol and 5 µL Nu-PAGE lithium dodecyl sulfate (LDS) sample buffer (Invitrogen), then heated at 98 °C for 30 min. Proteins were separated on 4–12% Bis-Tris gels (Invitrogen) alongside a PageRuler Plus Prestained Protein Ladder (Thermo Scientific). Electrophoresis was performed in MES-SDS buffer at 4 °C for 65 min at 110 V. Gels were stained with Imperial Protein Stain (Thermo Scientific) for 15 min, destained overnight, and imaged using a ChemiDoc MP system with Image Lab 5.2.1 software (Bio-Rad).

Dynamic light scattering (DLS)

S and VLP-S proteins were diluted in 100 µL of PBS so that the final solution contained 4 µg of S. MS2-SA was diluted in 100 µL of PBS so that the solution contained 3 µ g of the protein. The protein solution was added to a UVette (Eppendorf) and 13 acquisitions per sample were measured and displayed as % volume with a Zetasizer Nano (Malvern).

Analytical SEC

S and VLP-S proteins were diluted in 950 µL of PBS so that the final solution contained 8 µg of S. The solution was run on Superdex 200 Increase 10/300 Column (Cytiva) using the Unicorn 7 control system (Cytiva) and was eluted with 1 CV of PBS at 0.65 mL/minute. The absorbance at 210 nm was monitored during elution.

Phylogenetic tree

Spike protein amino acid sequences (Supplementary Table 2) were aligned using Clustal Omega 1.2.2. Pairwise amino acid identity percentages were calculated directly from this alignment. Phylogenetic relationships were inferred using PhyML v2012.04.12 (University of Montpellier) with a maximum parsimony starting tree and the LG amino acid substitution model. The SARS-CoV-2 spike protein (YP_009724390.1) was included as an outgroup to root the tree and subsequently removed for clarity. Trees were visualized with TreeViewer v2.2.0.

Antigenic cartography

Antigenic cartography was generated with IgG endpoint titer data using the Racmacs R package (Racmacs 1.1.35 with R 4.2.1 and RStudio 2022.07.01)[35,47]. The IgG endpoint titers from each serum sample against each viral antigen were used to calculate the dissimilarity value D_{ij} between each serum i and antigen j according to the equation $D_{ij} = -\log_2 H_{ij} + \log_2 H_{i,\max}$, where H_{ij} is the IgG endpoint titer of serum i against antigen j and $H_{i,\max}$ is the maximum titer observed for serum i. The error function for each serum-antigen pair was defined as $E_{ij} = (D_{ij} - d_{ij})^2$ with d_{ij} denoting the Euclidean distance between serum i and antigen j on the two-dimensional map. Conjugate gradient descent optimization was applied to minimize the total error, and 5000 restarts with randomized starting positions were performed to approximate the global optimum.

Biosafety and approvals

All experiments with MERS-CoV were conducted under biosafety level 3 agriculture (BSL-3 AG) containment at the Influenza Research Institute

using protocols approved by the University of Wisconsin–Madison Institutional Biosafety Committee. The facility is designed to meet or exceed the standards outlined in *Biosafety in Microbiological and Biomedical Laboratories*, 6th edition. All mouse studies were performed under protocol V006426 reviewed by the Institutional Animal Care and Use Committee at the University of Wisconsin-Madison.

Cell line and virus

MERS-CoV strain EMC/2012 (BEI Resources, NR-44260) was propagated in Vero E6/TMPRSS2 cells (Japanese Cancer Research Resources Bank, JCRB1819) maintained in high-glucose Dulbecco's modified Eagle's medium (DMEM) supplemented with 10% fetal bovine serum (FBS), antibiotic-antimycotic solution, and 1 mg/ml geneticin (G418; Invivogen). Vero E6/TMPRSS2 cells were tested monthly for mycoplasma contamination by PCR and consistently confirmed negative.

Animal care, immunizations, challenge studies, and antibody responses

Mice were maintained under standard conditions with *ad libitum* access to food, water, bedding, and enrichment. Rooms were kept at controlled temperature and humidity on a 12 h light/dark cycle. Animals were monitored at least once daily by trained personnel, and humane endpoints were applied for signs of severe infection. Group sizes were based on prior vaccine studies[32]; no statistical power calculations were performed. Blinding was not implemented, as all procedures were conducted under BSL-3 AG containment.

Groups of five female C57BL/6 mice (Jackson Laboratories) or hDPP4-Tg mice (colony established from 288/330 + /+ breeders kindly provided by Dr. Ralph Baric[38]), aged 6–8 weeks, were immunized subcutaneously under isoflurane anesthesia. Each animal received 125 µL formulations containing either 7.5 µg S displayed on VLP-S or the corresponding amount of VLP control, mixed 1:1 with an adjuvant formulation (Alhydrogel).

For immunogenicity studies, mice were bled under deep isoflurane anesthesia four weeks post-immunization. Heat-inactivated sera were analyzed by ELISA to determine antibody endpoint titers against the indicated viral S proteins. Virus neutralization assays were performed with MERS-CoV on Vero E6/TMPRSS2 cells using two-fold diluted serum samples with approximately 1000 pfu of virus. The virus and sera mixture was incubated at 37 °C for 30 min and then added to confluent Vero E6/TMPRSS2 cells that had been plated the day prior in 96-well plates. The cells were then incubated for 3 days at 37 °C. Virus neutralization titers were determined as the highest serum dilution that completely prevented CPE.

For challenge studies, hDPP4 mice were infected intranasally with 10^5 pfu of MERS-CoV while under isoflurane anesthesia, four weeks after immunization. At three days post-infection, mice were euthanized by isoflurane overdose, and lung and nasal turbinate tissues were collected. Viral titers were determined from clarified tissue homogenates applied to confluent Vero E6/TMPRSS2 cells overlaid with 1% methylcellulose.

Data availability

The data that supports the findings of this paper can be found within the manuscript and Supplementary Information. Unprocessed SDS-PAGE gel images for Fig. 2d are available in Supplementary Figure 1. Protein sequences for MS2-AviTag and the S proteins are available in Supplementary Table 1. NCBI and NGDC accession numbers for Fig. 1 are available in Supplementary Table 2. Source data for Fig. 2b, 2c, and 2e; Fig. 3b and 3d; Fig. 4b and 4c are available in the Supplementary Data No. 1 file.

Received: 15 December 2025; Accepted: 5 February 2026;
Published online: 19 February 2026

References

1. Zaki, A. M., Boheemen, S. V., Bestebroer, T. M., Osterhaus, A. D. M. E. & Fouchier, R. A. M. Isolation of a Novel Coronavirus from a Man with Pneumonia in Saudi Arabia. *N. Engl. J. Med.* **367**, 1814–1820 (2012).
2. Sikkema, R. S. et al. Global status of Middle East respiratory syndrome coronavirus in dromedary camels: a systematic review. *Epidemiol. Infect.* **147**, e84 (2019).
3. Folegatti, P. M. et al. Safety and immunogenicity of a candidate Middle East respiratory syndrome coronavirus viral-vectored vaccine: a dose-escalation, open-label, non-randomised, uncontrolled, phase 1 trial. *Lancet Infect. Dis.* **20**, 816–826 (2020).
4. Koch, T. et al. Safety and immunogenicity of a modified vaccinia virus Ankara vector vaccine candidate for Middle East respiratory syndrome: an open-label, phase 1 trial. *Lancet Infect. Dis.* **20**, 827–838 (2020).
5. Modjarrad, K. et al. Safety and immunogenicity of an anti-Middle East respiratory syndrome coronavirus DNA vaccine: a phase 1, open-label, single-arm, dose-escalation trial. *Lancet Infect. Dis.* **19**, 1013–1022 (2019).
6. Zhang, N. et al. Identification of an ideal adjuvant for receptor-binding domain-based subunit vaccines against Middle East respiratory syndrome coronavirus. *Cell. Mol. Immunol.* **13**, 180–190 (2016).
7. Wang, Y. et al. Receptor-binding domain of MERS-CoV with optimal immunogen dosage and immunization interval protects human transgenic mice from MERS-CoV infection. *Hum. Vaccines Immunotherapeutics* **13**, 1615–1624 (2017).
8. Tai, W. et al. A recombinant receptor-binding domain of MERS-CoV in trimeric form protects human dipeptidyl peptidase 4 (hDPP4) transgenic mice from MERS-CoV infection. *Virology* **499**, 375–382 (2016).
9. Tai, W. et al. Recombinant Receptor-Binding Domains of Multiple Middle East Respiratory Syndrome Coronaviruses (MERS-CoVs) Induce Cross-Neutralizing Antibodies against Divergent Human and Camel MERS-CoVs and Antibody Escape Mutants. *J. Virol.* **91**, e01651–01616 (2017).
10. Dai, L. et al. A Universal Design of Betacoronavirus Vaccines against COVID-19, MERS, and SARS. *Cell* **182**, 722–733.e711 (2020).
11. Wang, C. et al. Novel chimeric virus-like particles vaccine displaying MERS-CoV receptor-binding domain induce specific humoral and cellular immune response in mice. *Antivir. Res.* **140**, 55–61 (2017).
12. Kim, Y.-S. et al. Chaperna-Mediated Assembly of Ferritin-Based Middle East Respiratory Syndrome-Coronavirus Nanoparticles. *Front. Immunol.* **9 - 2018** (2018).
13. Okba, N. M. A. et al. Particulate multivalent presentation of the receptor binding domain induces protective immune responses against MERS-CoV. *Emerg. Microbes Infect.* **9**, 1080–1091 (2020).
14. Chao, C. W. et al. Protein nanoparticle vaccines induce potent neutralizing antibody responses against MERS-CoV. *Cell Reports* **43**, https://doi.org/10.1016/j.celrep.2024.115036 (2024).
15. Lin, L. C.-W. et al. Viromimetic STING Agonist-Loaded Hollow Polymeric Nanoparticles for Safe and Effective Vaccination against Middle East Respiratory Syndrome Coronavirus. *Adv. Funct. Mater.* **29**, 1807616 (2019).
16. Shehata, M. M. et al. Bacterial Outer Membrane Vesicles (OMVs)-Based Dual Vaccine for Influenza A H1N1 Virus and MERS-CoV. *Vaccines* **7**, 46 (2019).
17. Almansour, I. & Jermy, B. R. Nucleic acid vaccine candidates encapsulated with mesoporous silica nanoparticles against MERS-CoV. *Hum. Vaccines Immunotherapeutics* **20**, 2346390 (2024).
18. Tai, W. et al. MERS-CoV RBD-mRNA vaccine induces potent and broadly neutralizing antibodies with protection against MERS-CoV infection. *Virus Res.* **334**, 199156 (2023).
19. Shi, L. et al. A single-dose intranasal immunization with a novel bat influenza A virus-vectored MERS vaccine provides effective protection against lethal MERS-CoV challenge. *mBio* **16**, e01107–e01125 (2025).
20. Menachery, V. D. et al. Trypsin Treatment Unlocks Barrier for Zoonotic Bat Coronavirus Infection. *J. Virol.* **94**, https://doi.org/10.1128/JVI.01774-19 (2020).

21. Lau, S. K. P. et al. Receptor Usage of a Novel Bat Lineage C Betacoronavirus Reveals Evolution of Middle East Respiratory Syndrome-Related Coronavirus Spike Proteins for Human Dipeptidyl Peptidase 4 Binding. *J. Infect. Dis.* **218**, 197–207 (2018).
22. Park, Y.-J. et al. Molecular basis of convergent evolution of ACE2 receptor utilization among HKU5 coronaviruses. *Cell* **188**, 1711–1728.e1721 (2025).
23. Xiong, Q. et al. Close relatives of MERS-CoV in bats use ACE2 as their functional receptors. *Nature* **612**, 748–757 (2022).
24. Luo, C.-M. et al. Discovery of Novel Bat Coronaviruses in South China That Use the Same Receptor as Middle East Respiratory Syndrome Coronavirus. *J. Virol.* **92**, 00116–00118 (2018).
25. Tse, L. V. et al. A MERS-CoV antibody neutralizes a pre-emerging group 2c bat coronavirus. *Sci. Transl. Med.* **15**, eadg5567 (2023).
26. Chen, J. et al. A bat MERS-like coronavirus circulates in pangolins and utilizes human DPP4 and host proteases for cell entry. *Cell* **186**, 850–863.e816 (2023).
27. Xia, L. Y. et al. Isolation and characterization of a pangolin-borne HKU4-related coronavirus that potentially infects human-DPP4-transgenic mice. *Nat. Commun.* **15**, 1048 (2024).
28. Lau, S. K. P. et al. Isolation of MERS-related coronavirus from lesser bamboo bats that uses DPP4 and infects human-DPP4-transgenic mice. *Nat. Commun.* **12**, 216 (2021).
29. Yang, Y. et al. Receptor usage and cell entry of bat coronavirus HKU4 provide insight into bat-to-human transmission of MERS coronavirus. *Proc. Natl. Acad. Sci. USA* **111**, 12516–12521 (2014).
30. Wang, Q. et al. Bat origins of MERS-CoV supported by bat coronavirus HKU4 usage of human receptor CD26. *Cell Host Microbe* **16**, 328–337 (2014).
31. Hsieh, C.-L. et al. Stabilized coronavirus spike stem elicits a broadly protective antibody. *Cell Reports* **37**, https://doi.org/10.1016/j.celrep.2021.109929 (2021).
32. Halfmann, P. J. et al. Merbecovirus S2 subunit vaccines elicit cross reactive antibodies and provide partial protection against MERS coronavirus. *npj Viruses* **3**, 60 (2025).
33. Chiba, S. et al. Multivalent nanoparticle-based vaccines protect hamsters against SARS-CoV-2 after a single immunization. *Commun. Biol.* **4**, 597 (2021).
34. Halfmann, P. J. et al. Multivalent S2 subunit vaccines provide broad protection against Clade 1 sarbecoviruses in female mice. *Nat. Commun.* **16**, 462 (2025).
35. Halfmann, P. J. et al. Broad protection against clade 1 sarbecoviruses after a single immunization with cocktail spike-protein-nanoparticle vaccine. *Nat. Commun.* **15**, 1284 (2024).
36. Halfmann, P. J. et al. Multivalent S2-based vaccines provide broad protection against SARS-CoV-2 variants of concern and pangolin coronaviruses. *eBioMedicine* **86**, 104341 (2022).
37. Boon, A. C. M. et al. Recognition of Homo- and Heterosubtypic Variants of Influenza A Viruses by Human CD8+ T Lymphocytes1. *J. Immunol.* **172**, 2453–2460 (2004).
38. Cockrell, A. S. et al. A mouse model for MERS coronavirus-induced acute respiratory distress syndrome. *Nat. Microbiol* **2**, 16226 (2016).
39. Li, K. et al. Mouse-adapted MERS coronavirus causes lethal lung disease in human DPP4 knockin mice. *Proc. Natl. Acad. Sci.* **114**, E3119–E3128 (2017).
40. Harrer, C. E. et al. Identification of a Spike-Specific CD8+ T-Cell Epitope Following Vaccination Against the Middle East Respiratory Syndrome Coronavirus in Humans. *J. Infect. Dis.* **230**, e327–e332 (2024).
41. Weskamm, L. M. et al. Dissecting humoral immune responses to an MVA-vectored MERS-CoV vaccine in humans using a systems serology approach. *iScience* **27**, https://doi.org/10.1016/j.isci.2024.110470 (2024).
42. Schäfer, A. et al. Antibody potency, effector function, and combinations in protection and therapy for SARS-CoV-2 infection in vivo. *J. Exp. Med.* **218**, https://doi.org/10.1084/jem.20201993 (2021).
43. Mackin, S. R. et al. Fc-γR-dependent antibody effector functions are required for vaccine-mediated protection against antigen-shifted variants of SARS-CoV-2. *Nat. Microbiol* **8**, 569–580 (2023).
44. Liu, J. et al. CD8 T cells contribute to vaccine protection against SARS-CoV-2 in macaques. *Sci. Immunol.* **7**, eabq7647 (2022).
45. Pallesen, J. et al. Immunogenicity and structures of a rationally designed prefusion MERS-CoV spike antigen. *Proc. Natl. Acad. Sci.* **114**, E7348–E7357 (2017).
46. Fairhead, M., Krndija, D., Lowe, E. D. & Howarth, M. Plug-and-play pairing via defined divalent streptavidins. *J. Mol. Biol.* **426**, 199–214 (2014).
47. Smith, D. J. et al. Mapping the antigenic and genetic evolution of influenza virus. *Science* **305**, 371–376 (2004).

Acknowledgements

Y.K. and R.S.K. acknowledge support by the National Institute of Allergy and Infectious Diseases of the National Institutes of Health under Award Number P01 AI165077. R.S.K. acknowledges support from the Garry Betty/ V Foundation Chair Fund at the Georgia Institute of Technology. Y.K. acknowledges support from a Research Program on Emerging and Reemerging Infectious Diseases (JP21fk0108552 and JP21fk0108615), a Project Promoting Support for Drug Discovery (JP21nf0101632), the Japan Program for Infectious Diseases Research and Infrastructure (JP22wm0125002), and the University of Tokyo Pandemic Preparedness, Infection and Advanced Research Center (UTOPIA) grant (JP223fa627001) from the Japan Agency for Medical Research and Development. A.D. was supported in part by the T32 Research Training Program in Immunoengineering from the National Institute of Biomedical Imaging and Bioengineering of the National Institutes of Health (T32 EB021962). The content is solely the responsibility of the authors and does not necessarily represent the official views of the National Institutes of Health.

Author contributions

R.S.K., P.J.H., J.L., T.W., and A.D. conceptualized the project. P.J.H. and T.W. conducted in vivo experiments and titer assays. J.L. and A.D. produced the vaccines. J.L. characterized the vaccines, conducted formal analyses, and produced visualizations. A.D. designed the antigens. P.J.H., J.L., and T.W. were involved in data curation. R.S.K., J.L., and A.D. wrote the original manuscript. R.S.K., P.J.H., J.L., T.W., and A.D. edited the manuscript. R.S.K. and Y.K. provided supervision, project administration, and funding acquisition. All authors have read and approved the manuscript.

Competing interests

The authors declare no competing interests.

Additional information

Supplementary information The online version contains supplementary material available at https://doi.org/10.1038/s44298-026-00179-4.

Correspondence and requests for materials should be addressed to Yoshihiro Kawaoka or Ravi S. Kane.

Reprints and permissions information is available at http://www.nature.com/reprints

Publisher's note Springer Nature remains neutral with regard to jurisdictional claims in published maps and institutional affiliations.

Open Access This article is licensed under a Creative Commons Attribution-NonCommercial-NoDerivatives 4.0 International License, which permits any non-commercial use, sharing, distribution and reproduction in any medium or format, as long as you give appropriate credit to the original author(s) and the source, provide a link to the Creative Commons licence, and indicate if you modified the licensed material. You do not have permission under this licence to share adapted material derived from this article or parts of it. The images or other third party material in this article are included in the article's Creative Commons licence, unless indicated otherwise in a credit line to the material. If material is not included in the article's Creative Commons licence and your intended use is not permitted by statutory regulation or exceeds the permitted use, you will need to obtain permission directly from the copyright holder. To view a copy of this licence, visit http://creativecommons.org/licenses/by-nc-nd/4.0/.

© The Author(s) 2026